Strong Electron-Phonon Coupling in Yttrium under Pressure

Z. P. Yin, S. Y. Savrasov, and W. E. Pickett

Department of Physics, University of California, Davis, California, 95616

(Dated: August 13, 2006)

Linear response methods are applied to identify the increase in electron-phonon coupling in elemental yttrium that is responsible for its high superconducting critical temperature T_c, which reaches nearly 20 K at 115 GPa. While the evolution of the band structure and density of states is smooth and seemingly modest, there is strong increase in the $4d$ content of the occupied conduction states under pressure. We find that the transverse mode near the L point of the fcc Brillouin zone, already soft at ambient pressure, becomes unstable (in harmonic approximation) at a relative volume $V/V_o = 0.60$ ($P \approx 42$ GPa). The coupling to transverse branches is relatively strong at all high symmetry zone boundary points X, K, and L. Coupling to the longitudinal branches is not as strong, but extends over more regions of the Brillouin zone and involves higher frequencies. Evaluation of the electron-phonon spectral function $\alpha^2 F(\omega)$ shows a very strong increase with pressure of coupling in the 2-8 meV range, with a steady increase also in the 8-20 meV range. These results demonstrates strong electron-phonon coupling in this system that can account for the observed range of T_c.

I. INTRODUCTION

The remarkable discovery[1] in 2001 of MgB_2 with superconducting critical temperature T_c=40K, and the fact that the simple free-electron-like metal lithium[2–4] also has T_c in the 14-20K under 30-50 GPa pressure, has greatly increased efforts in seeking higher T_c in elements and simple compounds. Currently 29 elements are known to be superconducting at ordinary pressure and 23 other elements superconduct only under pressure[5,6]. Among elements there is a clear trend for those with small atomic number Z to have higher values of T_c, although much variation exists. For example, under pressure[7,8] Li, B, P, S, Ca, and V all have T_c in the range 11-20 K. Hydrogen[9–11], the lightest element, is predicted to superconduct at much higher temperature at pressures where it becomes metallic.

While light elements tend to have higher T_c among elemental superconductors, Hamlin *et al.*[12] recently reported that Y (Z=39) superconducts at T_c=17K under 89 GPa pressure and 19.5 K at 115 GPa, with the trend suggesting higher T_c at higher pressure. This result illustrates that heavier elements should not be neglected; note that La (Z=57) has T_c up to 13 K under pressure.[13,14] The superconductivity of La has been interpreted in terms of the rapidly increasing density of states of $4f$ bands near Fermi level with increasing pressure, causing phonon softening and resulting stronger coupling under pressure.[15,16] Such a scenario would not apply to Y, since there are no f bands on the horizon there. No full calculations of the phonon spectrum and electron-phonon coupling have been carried out for either Y or La to date.

La and Y are two of the few elemental transition metals to have T_c above[7,8] 10 K, and the case of Y is unusually compelling, since its value of T_c is at least as high that of Li, qualifying it as having the highest T_c of any elemental superconductor. Moreover, the reduced volume $v \equiv V/V_0$=0.42 corresponds to the value of $T_c \approx$ 20K in Y [12] (115 GPa) and also to the report of $T_c \approx$ 20K in (strained) Li [2] above 50 GPa.[17,18] For our study of Y reported here, it is first necessary to understand its phase diagram. Under pressure, it follows a structure sequence[19,20] through close-packed phases that is typical of rare earth metals: hcp→Sm-type→dhcp→dfcc (dfcc is distorted fcc, with trigonal symmetry). The transitions occur around 12 GPa, 25 GPa, and 30-35 GPa. Superconductivity was first found[21] in Y by Wittig in the 11-17 GPa range (1.2-2.8 K), in what is now known to be the Sm-type structure. From 33 GPa to 90 GPa T_c increases smoothly (in fact T_c increases linearly with decrease in v over the entire 35-90 GPa range[12]) suggesting that Y remains in the fcc phase, perhaps with the distortion in the dfcc phase vanishing (the tendency is for the c/a ratio in these structures to approach ideal at high pressure[19]). Calculations[22] predict it adopts the bcc structure at extremely high pressure(>280 GPa), but this is far beyond our interest here.

In this paper we report electronic structure and electron-phonon coupling calculations of Y for reduced volumes in the range $0.6 \leq v \leq 1$ (pressures up to 42 GPa). Our results indeed show strong electron-phonon coupling and phonon softening with increasing pressure. A lattice instability (in the harmonic approximation used in linear response calculations) is encountered at v=0.6 and persists to higher pres-

sures. The instability arises from the vanishing of the restoring force for transverse displacements for $Q\| < 111 >$ near the zone boundary, corresponding to sliding of neighboring close-packed layers of atoms. It is only the stacking sequence of these layers that distinguishes the various structures in the pressure sequence of structures (see above) that is observed in rare earth metals. Near-vanishing of the restoring force for sliding of these layers is consistent with several stacking sequences being quasi-degenerate, as the structural changes under pressure suggest.

This paper is organized as follows. In Sec. II structural details are given, and the calculational methods are described. Results for the electronic structure and its evolution with pressure are provided in Sec. III. The background for understanding the electron-phonon coupling calculations is provided in Sec. IV, and corresponding results are presented and analyzed in Sec. V. The implications are analyzed in Sec. VI.

II. STRUCTURE AND CALCULATION DETAILS

Yttrium crystallizes in the hcp structure at ambient pressure with space group $P63/mmc$ (#194) and lattice constants a=3.647 Å and c=5.731 Å[23].

Since the observed structures are all close packed (or small variations from) and above 35 GPa Y is essentially fcc, we reduce the calculational task by using the fcc structure throughout our calculations. The space group is $Fm3m$ (#225), with the equivalent ambient pressure lattice constant a=5.092 Å. We do note however that results for electron-phonon strength can be sensitive to the crystal symmetry, both through the density of states and through the nesting function that is described below.

We use the full potential local orbital (FPLO) code[24] to study the electronic structure, and apply the full-potential linear-muffin-tin-orbital (LM-TART) code[25] to calculate the phonon frequencies and the electron-phonon coupling spectral function $\alpha^2 F$. For FPLO, a k mesh of 36^3 and the Perdew-Wang (PW92)[26] parametrization of the Ceperley-Alder correlation potential are used. The basis set is 1s2s2p3s3p3d::(4s4p)/5s5p4d+. For LMTART, a k mesh of 48^3 and the Perdew-Burke-Ernzerhof generalized gradient approximation[27] for exchange-correlation potential are used. For the electron-phonon coupling calculations we used a phonon Q mesh of 16^3, which has 145 Q points in the irre-
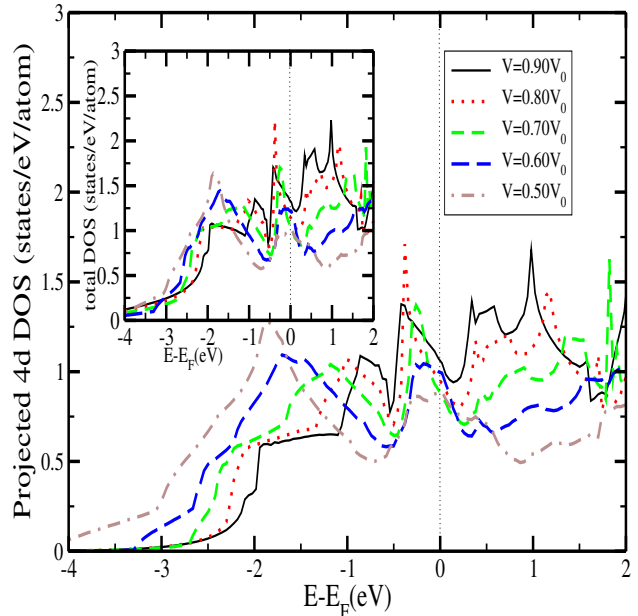

FIG. 1: (Color online) Plot of the total DOS and projected $4d$ DOS per atom of fcc Y with different volumes. Both the total and the $4d$ density of states at Fermi level decrease with reduction in volume.

ducible Brillouin zone.

III. ELECTRONIC STRUCTURE UNDER PRESSURE

Many studies suggest that the general character of an elemental rare earth metal is influenced strongly by the occupation number of the d electrons, which changes under pressure. Our calculations show that the $4d$ occupation number of trivalent Y increases from 1.75 at ambient pressure, to a little above 2 at V=0.7V$_0$ and then finally close to 3 at V=0.3V$_0$ (which is extreme pressure). Such an increase can be seen from the projected density of states (PDOS) of $4d$ states (Fig. 1) at different volumes. From Fig. 1 broadening of the density of states with reduction in volume can be seen, but is not a drastic effect. The main occupied $4d$ PDOS widens from 2 eV to 3 eV with reduction of the volume to v=0.5. The value of of the density of states at the Fermi level (taken as the zero of energy) $N(0)$ decreases irregularly with volume reduction; the values are given in Table I.

The pressure evolution of the band structure is indicated in Fig. 2, where the $4d$ character at v=1.00 (black) and v=0.50 (gray) is emphasized. First, the
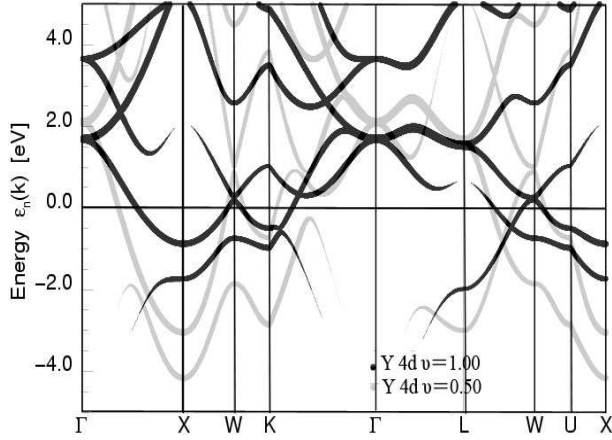
FIG. 2: (Color online) Plot along high symmetry directions of the bands of Y at V/V_o=1.00 and at V/V_o=0.50. The "fattening" of the bands is proportional to the amount of Y $4d$ character. Note that the $4d$ character goes substantially in the occupied bands under pressure (the lighter shading), although there is relatively little change in the Fermi surface band crossings.

relative positions of the Fermi level crossings change smoothly, indicating there is little change in the Fermi surface topology. This slow change is also seen in Fermi surface plots, of which we show one (below). Second, the overall band widths change moderately, as was noted above in the discussion of the density of states. The change in position of $4d$ character is more substantial, however. $4d$ bands at X lying at -1 eV and -2 eV at ambient volume are lowered to -3 eV and -4 eV at v=0.50. Lowering of $4d$ character bands at K and W is also substantial. Thus Y is showing the same trends as seen in alkali metals. For Cs and related alkalies and alkaline earths under pressure, $6s$ character diminishes as $5d$ character grows strongly with pressure.[28] In Li, $2s$ character at the Fermi surface evolves to strong $2p$ mixture[29] at the volume where T_c goes above 10 K.

The Fermi surface of Y at ambient pressure (hcp) has been of interest for some time, from the pioneering calculation of Loucks[30] to the recent measurements and calculations of Crowe *et al.*[31] However, the unusual Fermi surface in the hcp structure (having a single strong nesting feature) is nothing like that in the fcc phase we are addressing, which is unusual in its own way. At v=1.00 the fcc Fermi surface is a large 'belly' connected by wide necks along $< 111 >$ directions as in Cu, but in addition there are tubes ('wormholes') connecting a belly to a neighboring zone's belly through each of the 24 W
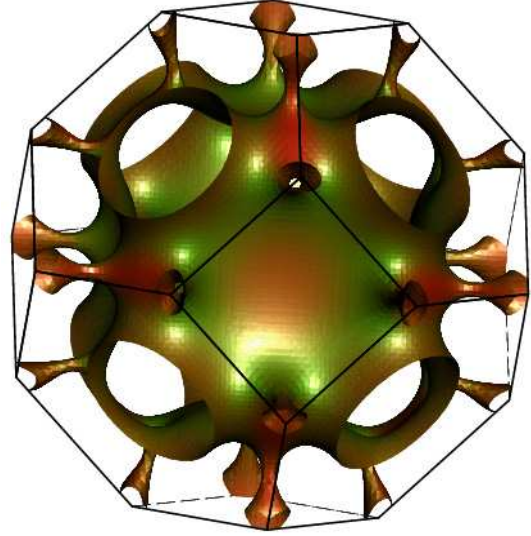

FIG. 3: (Color online) Surface plot of the Fermi surface of fcc Y at a volume corresponding to ambient pressure. The surface is shaded according to the Fermi velocity, with the minimum $(2.4 \times 10^7$ cm/s) and maximum $((5.8 \times 10^7$ cm/s) denoted by the green (dark, around the dimples) and red (belly regions), respectively. The surface is isomorphic to that of Cu, *except* for the tubes through the W point vertices that connect Fermi surfaces in neighboring Brillouin zones. The evolution with pressure is described in the text.

points. The belly encloses holes rather than electrons as in Cu; that is, the electrons are confined to a complex multiply-connected web enclosing much of the surface of the Brillouin zone.

As the volume is reduced, the wormholes slowly grow in diameter until in the range $0.5< v <0.6$, they merge in certain places with the necks along the $< 111 >$ directions, and the change in topology leaves closed surfaces around the K points as well as a different complex multiply-connected sheet. The point we make is that, at all volumes, the Fermi surface is very complex geometrically. There is little hope of identifying important "nesting" wavevectors short of an extensive calculation. Even for the simple Fermi surface of fcc Li, unexpected nesting vectors were located[29] in three high symmetry planes of the zone. The rest of the zone in Li still remains unexplored.

IV. BACKGROUND: ELECTRON-PHONON COUPLING

The electron-phonon spectral function $\alpha^2 F(\omega)$ can be expressed in terms of phonon properties [and $N(0)$] in the form[32]

$$\alpha^2 F(\omega) = \frac{1}{2\pi N(0)} \sum_{\mathbf{Q}\nu} \frac{\gamma_{\mathbf{Q}\nu}}{\omega_{\mathbf{Q}\nu}} \delta(\omega - \omega_{\mathbf{Q}\nu}) \quad (1)$$

where

$$F(\omega) = \sum_{\mathbf{Q}\nu} \delta(\omega - \omega_{\mathbf{Q}\nu}) \quad (2)$$

is the density of phonon states, and $N(0)$ is the single spin Fermi surface density of states. The phonon linewidth $\gamma_{\mathbf{Q}\nu}$ is given by

$$\gamma_{\mathbf{Q}\nu} = 2\pi\omega_{\mathbf{Q}\nu} \sum_{\mathbf{k}} |M^{[\nu]}_{\mathbf{k}+\mathbf{Q},\mathbf{k}}|^2 \delta(\varepsilon_{\mathbf{k}}) \delta(\varepsilon_{\mathbf{k}+\mathbf{Q}}) \quad (3)$$

where $M^{[\nu]}_{\mathbf{k}+\mathbf{Q}}$ is the electron-phonon matrix element; ν is the branch index. Sums over $\mathbf{Q}$ or $\mathbf{k}$ are conventionally normalized (divided by the number of unit cells in the normalization volume).

The quantities thus defined enable one to identify the contribution to λ from each mode, the "mode λ", as

$$\lambda_{\mathbf{Q}\nu} = \frac{2}{\omega_{\mathbf{Q}\nu} N(0)} \sum_{\mathbf{k}} |M^{[\nu]}_{\mathbf{k},\mathbf{k}+\mathbf{Q}}|^2 \delta(\varepsilon_{\mathbf{k}}) \delta(\varepsilon_{\mathbf{k}+\mathbf{Q}}) \quad (4)$$

With this definition λ is the average over the zone, and sum (not average) over the $N_\nu = 3$ branches of all of the $\lambda_{\mathbf{Q}\nu}$ values. The electron-phonon coupling strength λ then is given by

$$\lambda = \frac{4}{\pi N(0)} \sum_{\mathbf{Q}\nu} \frac{\gamma_{\mathbf{Q}\nu}}{\omega_{\mathbf{Q}\nu}^2} \equiv \sum_{\mathbf{Q}\nu} \lambda_{\mathbf{Q}\nu}. \quad (5)$$

The critical temperature T_c can be obtained by using the Allen-Dynes modification of the McMillan formula,[33,34] which depends on the logarithmic, first, and second frequency moments ω_{log}, $\omega_1 \equiv <\omega>$, and $\omega_2 \equiv <\omega^2>^{1/2}$, as well as λ and the Coulomb pseudopotential μ^*. For completeness, the expressions are provided in the Appendix. These averages are weighted according to the normalized coupling 'shape function' $2\alpha^2 F(\omega)/(\lambda\omega)$. They are often, and will be for Y especially under pressure, much different from simple averages over the spectrum $F(\omega)$.

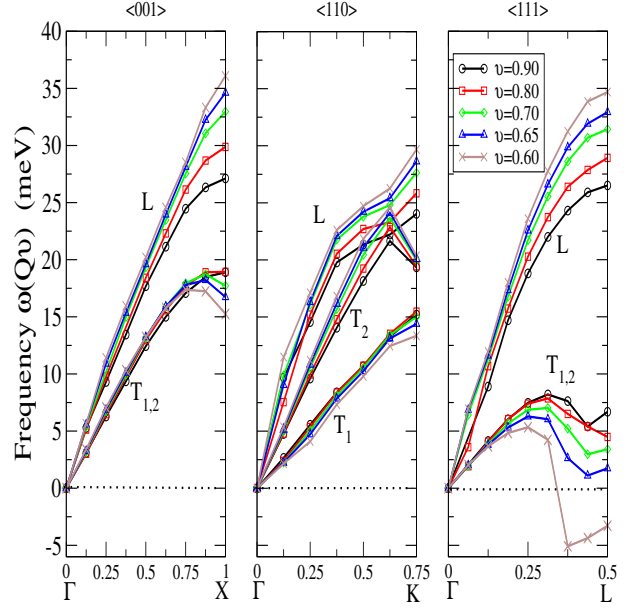Note that $\lambda_{\mathbf{Q}\nu}$, or $\gamma_{\mathbf{Q}\nu}$, incorporates a phase space factor, the 'nesting function'[29] $\xi(\mathbf{Q})$ describing the phase space that is available for electron-hole scattering across the Fermi surface(E_F=0),

$$\xi(\mathbf{Q}) = \frac{1}{N} \sum_{\mathbf{k}} \delta(\varepsilon_{\mathbf{k}}) \delta(\varepsilon_{\mathbf{k}+\mathbf{Q}}) \propto \oint_{\mathcal{L}} \frac{d\mathcal{L}_{\mathbf{k}}}{|\mathbf{v}_{\mathbf{k}} \times \vec{v}_{\mathbf{k}+\mathbf{Q}}|}. \quad (6)$$

Here $\mathcal{L}$ is the line of intersection of an undisplaced Fermi surface and one displaced by $\mathbf{Q}$, and $\vec{v}_k$ is the electron velocity at $\vec{k}$. These equations presume the adiabatic limit, in which the phonon frequencies are small compared to any electronic energy scale. This limit applies to elemental Y.

FIG. 4: (Color online) Plot of the calculated phonon spectrum along high symmetry directions (Γ-X, Γ-K, Γ-L) of fcc Y with different volumes. The longitudinal mode phonons increases with the distance from Γ points along all the three directions. Along Γ-X direction (left panel), the doubly degenerate traverse mode slightly softens near X point, while along Γ-K direction (left panel, only the T_2 mode sightly softens near K point. Along Γ-L direction (right panel), the already soft doubly degenerate transverse mode soften further near the L point with decreasing volume. At $V = 0.6V_0$, the frequency at L becomes imaginary, indicating lattice instability.

V. RESULTS AND ANALYSIS

A. Behavior of Phonons

The calculated phonon branches are shown along the high symmetry lines, from v=0.90 down to v=0.60, in Fig. 4. The longitudinal modes behave normally, increasing monotonically in frequency by $\sim$ 30% in this range. The transverse modes along $< 100 >$ and $< 110 >$ show little change; the doubly degenerate transverse mode at X *softens* by 20%, reflecting some unusual coupling. Along $< 110 >$, T_1 and T_2 denote modes polarized in the $x-y$ plane, and along the z axis, respectively.

The interesting behavior occurs for the (doubly degenerate) transverse branch along $< 111 >$. It is quite soft already at v=0.9 (7 meV, only 25% of the longitudinal branch), softer than the corresponding mode in hcp Y at ambient pressure.[35] With decreasing volume it *softens* monotonically, and becomes unstable between v=0.65 and v=0.60. It should not be surprising that the transverse mode at the L point is soft in a rare earth metal. The sequence of structural transitions noted in the introduction (typically hcp→Sm-type→dhcp→dfcc for trivalent elements) involves only different stacking of hexagonal layers of atoms along the cubic (111) direction. So although these various periodic stackings will have similar energies, the soft (becoming unstable) transverse mode at L indicates also that the barrier against sliding of these planes of atoms is very small. At v=0.60 (see Fig. 4) the largest instability is not at L itself but one-quarter of the distance back toward Γ. At v=0.65 there are surely already anharmonic corrections to the lattice dynamics and coupling from the short wavelength transverse branches.

B. Linewidths

The linewidths $\gamma_{Q\nu}$, one indicator of the mode-specific contribution to T_c, are shown in Fig. 5. To understand renormalization, one should recognize that in lattice dynamical theory it is ω^2, and not ω itself, that arises naturally. At v=0.90, ω^2 for the T modes is only 1/16 of the value for the longitudinal mode at the L point. A given amount of coupling will affect the soft modes much more strongly than it does the hard modes.

For the $< 110 >$ direction, the strong peak in $\gamma_{Q\nu}$ for the T_2 $\hat{z}$ polarized) mode at the zone boundary point K (5.7 meV) is reflected in the dip in this mode at K that can be seen in Fig. 4. At
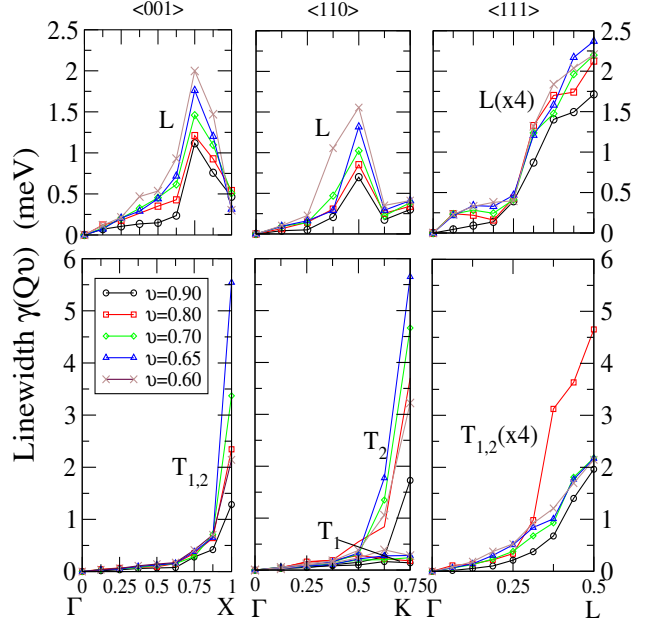

FIG. 5: (Color online) Plot of the calculated linewidths of fcc Y for varying volumes. The linewidths of the transverse modes at the X point increases from 1.3 to 5.5 as volume decreases from V=0.9V$_0$ to V=0.6V$_0$. The linewidths of the T_2 along $< 110 >$ modes show the same increase. The linewidths along the $< 111 >$ direction have been multiplied by four for clarity.

v=0.60 the linewidth is 1/3 of the frequency. The coupling to the T_1 mode along this line is negligible. Note that it is the T_1 mode that is strongly coupled in Li and is the first phonon to become unstable. A peak in the linewidth of the L modes correlates with a depression of the frequency along this line. Along $< 001 >$ the T modes again acquire large linewidths near the zone boundary under pressure. This electron-phonon coupling is correlated with the dip in the T frequency in the same region.

The coupling along the $< 111 >$ direction is not so large, either for T or for L branches (note, they have been multiplied by a factor of four in Fig. 5. The coupling is strongest at the zone boundary, and coupled with the softness already at v=0.90, the additional coupling causes an instability when the volume is reduced to v=0.60 (P = 42 GPa). This seems to represent an example where a rather modest amount of coupling has a potentially catastrophic result: instability of the crystal. Evidently Y is stabilized in the fcc structure by anharmonic effects, coupled with the fact that it is already close-packed.
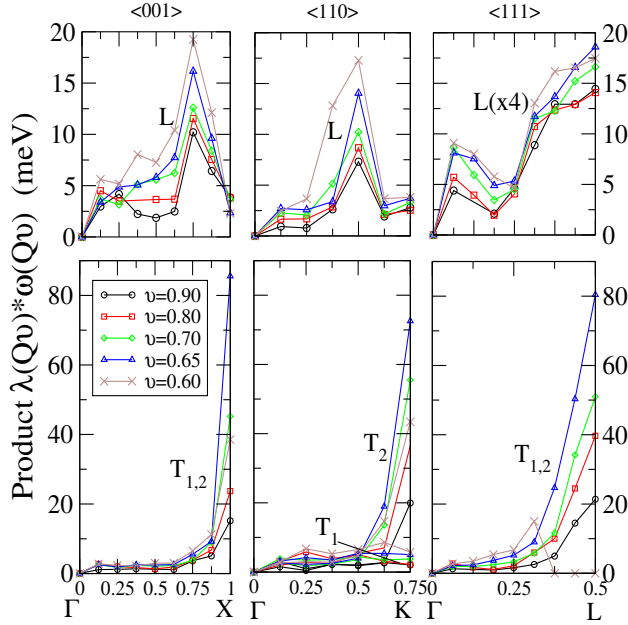
FIG. 6: (Color online) Plot of the product $\lambda_{Q\nu}\omega_{Q\nu}$ of fcc Y for different volumes, along the high symmetry directions. Note that the longitudinal (L) values along $< 111 >$ have been multiplied by four for clarity. In addition, values corresponding to unstable modes near L have been set to zero. Differences in this product reflect differences in matrix elements; see text.

C. Coupling Strength

It is intuitively clear that strong coupling to extremely low frequency modes is not as productive in producing high T_c as coupling to higher frequency modes. This relationship was clarified by Bergmann and Rainer,[36] who calculated the functional derivative $\delta T_c/\delta\alpha^2F(\omega)$. They found that coupling at frequencies less than $\bar{\omega} = 2\pi T_c$ has little impact on T_c (although coupling is never harmful). Since we are thinking in terms of Y's maximum observed $T_c \approx 20$ K, this means that coupling below $\bar{\omega} = 10$ meV becomes ineffective.

The product $\lambda_{Q\nu}\omega_{Q\nu} \propto \gamma_{Q\nu}/\omega_{Q\nu}$ gives a somewhat different indication of the relative coupling strength[37] than does either $\lambda_{Q\nu}$ or $\gamma_{Q\nu}$. It is also, up to an overall constant, just the nesting function defined earlier, with electron-phonon matrix elements included within the sum. Since the nesting function is a reflection of the phase space for scattering, it is independent of the polarization of the mode, hence differences between the three branches are due solely to the matrix elements.

TABLE I: For each volume v studied, the columns give the experimental pressure[22](GPa), the Fermi level density of states N(0) (states/Ry spin), and calculated values of the mean frequency $\omega_1 =< \omega >$ (meV), the logarithmic moment ω_{log} and second moment $\omega_2 =< \omega^2 >^{1/2}$ (all in meV), the value of λ, the product $\lambda\omega_2^2$ (meV^2), and T_c (K). For T_c the value of the Coulomb pseudopotential was taken as μ^*=0.15.

v	P	N(0)	ω_{log}	ω_1	ω_2	λ	$\lambda\omega_2^2$	T_c
0.90	6	9.7	12.5	13.6	14.7	0.75	162	4.0
0.80	14	11.3	11.6	13.2	14.5	1.30	273	11.9
0.70	26	9.1	10.1	12.0	13.8	1.53	291	13.0
0.65	32	8.4	7.6	10.2	12.6	2.15	341	14.4
0.60	42	7.9	6.9	9.5	12.1	2.80	410	(16.9)

This product $\lambda_{Q\nu}\omega_{Q\nu}$ is shown in Fig. 6. The weight in the transverse modes is concentrated near the zone boundary, with the region being broader around L than at X or K and growing in width with pressure. The T_1 branch along $< 110 >$, which is polarized along $[1\bar{1}0]$, shows essentially no coupling. The weight in this product for the longitudinal modes is peaked *inside* the zone boundary along the $< 001 >$ and $< 110 >$ directions with a mean value of 8-8 meV, and is weaker along the $< 111 >$ direction.

D. $\alpha^2F(\omega)$

The results for α^2F are displayed in Fig. 7. The longitudinal peak in the 20-35 range hardens normally with little change in coupling strength. The 8-20 meV range of transverse modes at v=0.90 increases in width to 2-24 meV at v=0.60, and the strength increases monotonically and strongly. The strong peak in $\alpha^2(\omega) = \alpha^2F(\omega)/F(\omega)$, shown in the bottom panel of Fig. 7, reflects the very soft modes that have been driven into the 2-5 meV range, and the fact that they are very relatively strongly coupled. The substantial increase in coupling, by a factor of $\sim$2.5, in the range 8-25 meV is important for T_c, as noted in the next subsection.

E. Estimates of T_c

This background helps in understanding the trends displayed in Table I, where T_c from the Allen-Dynes equation[33] (choosing the standard value of μ^*=0.15) and the contributing materials constants are displayed. The calculated values of λ increases
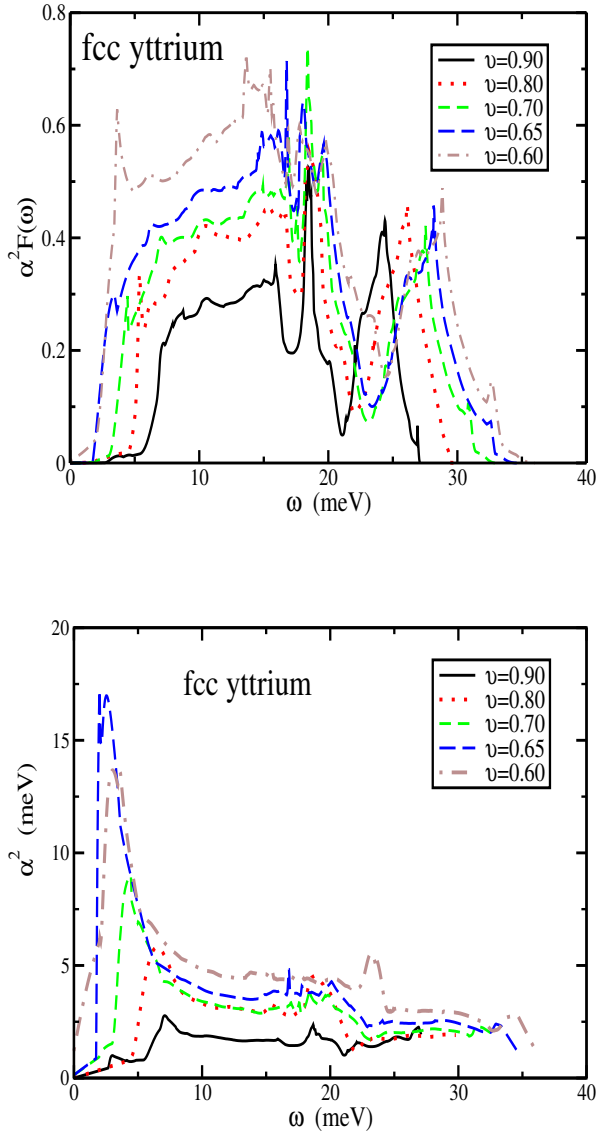
FIG. 7: (Color online) Top panel: Plot of $\alpha^2 F(\omega)$ versus ω As volume decreases, $\alpha^2 F(\omega)$ increases and gradually transfers to low frequency. Bottom panel: the frequency-resolved coupling strength $\alpha^2(\omega)$ for each of the volumes studied. The evolution with increased pressure is dominated by strongly enhanced coupling at very low frequency (2-5 meV).

strongly, by a factor of 3.7 in the volume range we have studied. Between $v=0.65$ and $v=0.60$ (the unstable modes are removed from consideration) λ increases 30% but T_c increases by only 2.5 degrees. The cause becomes clear in looking at the frequency moments. These moments are weighted by $\alpha^2 F(\omega)/\omega$. $\alpha^2(\omega)$ itself become strongly peaked

at low frequency under pressure, and it is further weighted by ω^{-1}. The frequency moments set the scale for T_c (ω_{log} in particular) and they *decrease* strongly with decreasing volume. In particular, ω_{log} decreases by 45% over the range of volumes we have studied, reflecting its strong sensitivity to soft modes.

Although the very low frequency peak in $\alpha^2(\omega)$ shown in Fig. 7 is impressive, the increase in T_c owes more to the increase in coupling strength in the 8-25 meV range, which is roughly a factor of 2.5. Leavens and Carbotte showed[38] that for some representative systems with $1.3 \leq \lambda \leq 3.3$, $T_c = 0.074$ $\lambda\omega_1$ works reasonably well; $\lambda\omega_1/2$ is just the integral of $\alpha^2 F$ ("area under $\alpha^2 F$"). The increase in the area under the $\alpha^2 F$ curve in Fig. 7 in the 8-25 meV regime is about double the increase in the range 0-8 meV. Restated, the very low frequency peak in $\alpha^2 F$ certainly contributes strongly to λ, but is also very effective in lowering the temperature scale (ω_{log}), and the product $\lambda\omega_1$ is more meaningful than λ.

Thus for $\alpha^2(\omega)$ shapes such as we find for Y, the quantities λ and ω_{log} which go into the Allen-Dynes equation for T_c do not provide a very physical picture of the change in T_c. For this reason we provide also in Table I the product $\lambda\omega_2^2 = N(0) < I^2 > /M$ ($< I^2 >$ is the conventional Fermi surface average of square of the electron-ion matrix element and M is the atomic mass). For the volumes $0.60 \leq v \leq 0.80$ in the table, the ratio of $\lambda\omega_2^2/T_c$ is nearly constant[37] at 23 ± 1.5 (in the units of the table), illustrating the strong cancellation of the increase of λ with the decrease in frequency moments in producing the resulting T_c.

VI. DISCUSSION

In this paper we have presented the evolution of elemental Y over a range of volumes ranging from low pressure to 42 GPa pressure ($V/V_o = 0.60$). Lattice instabilities that emerge near this pressure (and persist to higher pressures) make calculations for smaller volumes/higher pressures unrealistic. For simplicity in observing trends the structure has been kept cubic (fcc); however, the observed phases are all close-packed so it was expected that this restriction will still allow us to obtain the fundamental behavior underlying the unexpectedly high T_c in Y. On the other hand, the Fermi surface geometry varies strongly with crystal structure, and both the nesting function $\xi(Q)$ and the matrix elements will have some sensitivity to the type of long-range periodic-

ity.

In addition to the band structure, Fermi surface, and electronic density of states, we have also presented the phonon dispersion curves and linewidths along the high symmetry directions, and also have presented $\alpha^2 F(\omega)$ and the resulting value of T_c. The results show indeed that Y under pressure becomes a strongly coupled electron-phonon system, readily accounting for value of T_c in the range that is observed.

In spite of having used a relatively dense mesh of Q points for the phonons, it is clear that this Brillouin zone integral is still not well converged. Evaluation of $\xi(Q)$ on a very fine Q mesh in three planes for fcc Li, which has a very simple Fermi surface, has shown[29] that this nesting factor contains (thickened) surfaces of fine structure with high intensity. The convergence of this zone integral (and for example the resulting $\alpha^2 F$ function) has rarely been tested carefully in full linear response evaluations of phonons; such a test would be computationally intensive. Nevertheless, the general finding of strong coupling is clear.

Very recently it has been found that isovalent Sc is superconducting at 8.1 K under 74 GPa pressure.[39] Note that if the lattice were harmonic and the only difference between Sc and Y were the masses (which differ by a factor of two), T_c = 20 K for Y would translate to T_c = 28 K for Sc. (For an element with a harmonic lattice, λ is independent of mass.) The corresponding argument for (again isovalent) La gives T_c = 16 K. La has T_c = 13 K at 15 GPa, and has not been studied beyond[7] 45 GPa.

Another comparison may be instructive. Dynes and Rowell obtained and analyzed tunneling data[40] on Pb-Bi alloys where λ is well into the strong coupling region, becoming larger than two as is the case for Y under pressure in Table I. The $Pb_{0.65}Bi_{0.35}$ alloy has λ=2.13, $<\omega^2>$=22.6 meV^2. We can compare directly with the v=0.65 case in Table I, which has λ=2.15, $<\omega^2>$=159 meV^2. The product $M<\omega^2>$ for Y is three times as large as for the heavy alloy. Since the λ's are equal, the value of $N(0)<I^2>$ (equal to $\lambda M<\omega^2>$) is also three times as large as in the alloy. The values of T_c are 14.4 K (Y) and 9 K (alloy) [somewhat different values of μ^* were used.] The values of ω_{log} differ by less than a factor of two, due to the low-frequency coupling in $\alpha^2(\omega)$ in Y that brings that frequency down, and that is why the values of T_c also differ by less than a factor of two.

While this study is in some sense a success, in that it has become clear that strong electron-phonon coupling can account for the remarkable superconductivity of Y under pressure, there remains a serious shortcoming, one that is beyond the simple lack of numerical convergence that would pin down precisely λ, T_c, etc. What is lacking is even a rudimentary physical picture for what distinguishes Y and Li (T_c around 20 K under pressure) from other elemental metals which show low, or vanishingly small, values of T_c.

The rigid muffin-tin approximation (RMTA) of Gaspari and Gyorffy,[41] which approximates the phonon-induced change in potential and uses an isotropic idealization for the band structure to derive a simple result, seemed fairly realistic for the electronic contribution (the Hopfield η) for transition metal elements and intermetallics.[42,43] On top of these idealizations, there is an additional uncertainty in $<\omega^2>$ that must be guessed to obtain λ and T_c. One would not 'guess' the values of the frequency moments that we have obtained for Y under pressure.

In addition, the RMTA expression does not distinguish between the very different matrix elements for the various branches, giving only a polarization and Fermi surface average. Nevertheless, it gave a very useful understanding of trends[42] in electron-phonon coupling in elemental transition metals and in some intermetallic compounds. While the linear response evaluation of the phonon spectrum and the resulting coupling seems to work well, this more detailed approach has not yet provided – even for elemental superconductors – the physical picture and simple trends that would enable us to claim that we have a clear understanding of strong coupling superconductivity.

VIII. APPENDIX

We have obtained T_c using the Allen-Dynes equation

$$T_c = \frac{\omega_{log}}{1.2} f_1 f_2 exp\{-\frac{1.04(1+\lambda)}{\lambda - \mu^*(1+0.62\lambda)}\} \qquad (7)$$

where f_1 and f_2 contain the strong coupling corrections that are important for λ greater than unity (especially for λ=2.15 and 2.80 in Table I) but have little effect for $\lambda \sim 1$ or less. They are given by

$$f_1 = [1+(\lambda/\Lambda_1)^{3/2}]^{1/3}, \qquad (8)$$
$$f_2 = 1 + \frac{(\omega_2/\omega_{log}-1)\lambda^2}{\lambda^2 + \Lambda_2^2}, \qquad (9)$$

with

$$\Lambda_1 = 2.46(1+3.8\mu^*), \qquad (10)$$
$$\Lambda_2 = 1.82(1.6.3\mu^*)(\omega_2/\omega_{log}) \qquad (11)$$

depending on the Coulomb pseudopotential μ^* and the shape of $\alpha^2 F$ represented by ω_2/ω_{log}.

In terms of the normalized weighting function that arises in Eliashberg theory,

$$g(\omega) \equiv \frac{2}{\lambda\omega}\alpha^2 F(\omega) \qquad (12)$$

the (coupling-weighted) phonon moments are defined as

$$\omega_n \equiv [\ \int_0^\infty g(\omega)\omega^n]^{1/n} \qquad (13)$$

and

$$\omega_{log} \equiv lim_{n\rightarrow 0}\omega_n = exp[\ \int_0^\infty g(\omega)ln\omega]. \qquad (14)$$

[1] H. Nagamatsu, N. Nakagawa, T. Muranaka, Y. Zenitani, and J. Akimitsu, Nature (London) **410**, 63 (2001).

[2] K. Shimizu, H. Kimura, D. Takao, and K. Amaya, Nature **419**, 597 (2002).

[3] V. V. Struzhkin, M. I. Eremets, W. Gan, H.-K. Mao, and R. J. Hemley, Science **298**, 1213 (2002).

[4] S. Deemyad and J. S. Schilling, Phys. Rev. Lett. **91**, 167001 (2003).

[5] N. W. Ashcroft, Nature **419**, 569 (2002)

[6] M. I. Eremets, V. V. Struzhkin, H.-K. Mao, R. J. Hemley, Physica B **329-333**, 1312 (2003).

[7] J. S. Schilling, in *Treatise on High Temperature Superconductivity*, edited by J. R. Schrieffer (Springer-Verlag, Hamburg, 2006); cond-mat/0604090.

[8] C. Buzea and K. Robbie, Semicond. Sci. Technol. **18**, R1 (2005) and reference therein.

[9] N. W. Ashcroft, Phys. Rev. Lett. **21**, 1748 (1968).

[10] K. A. Johnson, N. W. Ashcroft, Nature **403**, 632 (2003).

[11] M. Stadele, R. M. Martin, Phys. Rev. Lett. **84**, 6070 (2000).

[12] J. J. Hamlin, V. G. Tissen, and J. S. Schilling, Phys. Rev. B **73**, 094522 (2006).

[13] H. Balster and J. Wittig, J. Low Temp. Phys. **21**, 377 (1975).

[14] V. G. Tissen, E. G. Ponyatovskii, M. V. Nefedova, F. Porsch, and W. B. Holzapfel, Phys. Rev. B **53**, 8238 (1996).

[15] W. E. Pickett, A. J. Freeman, D. D. Koelling, Phys. Rev. B **22**, 2695 (1980) and reference therein.

[16] H. Wühl, A. Eichler, and J. Wittig, Phys. Rev. Lett. **31**, 1393 (1973).

[17] M. Hanfland, I. Loa, K. Syassen, U. Schwarz, and K. Takemura, Solid State Commun. **112**, 123 (1999).

[18] M. Hanfland, K. Syassen, N. E. Christensen, and D. L. Novikov, Nature **408**, 174 (2000).

[19] Y. K. Vohra, H. Olijnik, W. Grosshans, and W. B. Holzapfel, Phys. Rev. Lett. **47**, 1065 (1981) and references therein.

[20] W. A. Grosshans and W. B. Holzapfel, Phys. Rev. B **45**, 5171 (1992).

[21] J. Wittig, Phys. Rev. Lett. **24**, 812 (1970).

[22] J. Melsen, J. M. Wills, B. Johansson and O. Eriksson, Phys. Rev. B **48**, 15574 (1993).

[23] F. H. Spedding, A. H. Daane and K. W. Herrmann, Acta Cryst. **9**, 599 (1956).

[24] K.Koepernik and H.Eschrig, Phys. Rev. B **59**, 1743 (1999).

[25] S. Y. Savrasov, Phys. Rev. B **54**, 16470 (1996);S. Y. Savrasov, D. Y. Savrasov, *ibid* **54** 16487 (1996).

[26] J. P. Perdew and Y. Wang, Phys. Rev. B **45**, 13244 (1992).

[27] J. P. Perdew, K. Burke, and M. Ernzerhof, Phys. Rev. Lett. **77**, 3865 (1996).

[28] M. Ross and A. K. McMahan, Phys. Rev. B **26**, 4088 (1982).

[29] D. Kasinathan, J. Kuneš, A. Lazicki, H. Rosner, C. S. Yoo, R. T. Scalettar, and W. E. Pickett, Phys. Rev. Lett. **96**, 047004 (2006).

[30] T. L. Loucks, Phys. Rev. **144**, 504 (1968).

[31] S. J. Crowe, S. B. Dugdale, Zs. Major, M. A. Alam, J. A. Duffy and S. B. Palmer, Europhys. Lett. **65**, 235 (2004).

[32] P. B. Allen, Phys. Rev. B **6**, 2577 (1972).

[33] P. B. Allen and R. C. Dynes, Phys. Rev. B **12**, 905 (1975).

[34] W. L. McMillan, Phys. Rev. **167**, 331 (1968).

[35] S. K. Sinha, T. O. Brun, L. D. Muhlestein, and J. Sakurai, Phys. Rev. B **1**, 2430 (1970).

[36] G. Bergmann and D. Rainer, Z. Physik A **263**, 59 (1973).

[37] Carbotte has argued that $\lambda\omega^2$ may be an even better indication of the coupling strength; see J. P. Carbotte, Rev. Mod. Phys. **62**, 1067 (1990) and references therein.

[38] C. R. Leavens and J. P. Carbotte, J. Low Temp. Phys. **14**, 195 (1974).

[39] J.J. Hamlin and J.S. Schilling, unpublished.

[40] R. C. Dynes and J. M. Rowell, Phys. Rev. B **11**, 1884 (1975).

[41] G. Gaspari and B. L. Gyorffy, Phys. Rev. Lett. **28**, 801 (1972).

[42] D. A. Papaconstantopoulos, L. L. Boyer, B. M. Klein, A. R. Williams, V. L. Morruzzi, and J. F. Janak, Phys. Rev. B **15**, 4221 (1977).

[43] W. E. Pickett, Phys. Rev. B **25**, 745 (1982).